NASA Technical Paper 3226

Effect of Temperature and Gap Opening Rate on the Resiliency of Candidate Solid Rocket Booster O-Ring Materials

Cynthia L. Lach

June 1992

Abstract

As a part of the redesign of the Space Shuttle solid rocket motor following the Challenger accident, the field and nozzle-to-case joints were designed to minimize gap opening caused by internal motor pressurization during ignition. The O-ring seals and glands for these joints were designed both to accommodate structural deflections and to promote pressure-assisted sealing. The resiliency behavior of several candidate O-ring materials was evaluated for the effects of temperature and gap opening rates. The performance of three of the elastomeric materials was tested under the specific redesign gap opening requirement. Dynamic flexure conditions unique to launch produce low-frequency vibrations in the gap opening. The effect of these vibrations on the ability of the O-ring to maintain contact with the sealing surface was also addressed.

The resiliency of the O-ring materials was found to be extremely sensitive to variations in temperature and gap opening rate. The top three elastomeric materials tracked the simulated solid rocket booster (SRB) field joint deflection at 75°F and 120°F. The external tank/SRB attach strut load vibrations had a negligible effect on the ability of the O-ring to track the simulated SRB field joint deflection.

Introduction

The Space Shuttle solid rocket booster (SRB) is composed of separate steel segments that are 12-ft-diameter cylindrical shells (see fig. 1(a)). Before the Challenger accident, the adjoining case segments were mechanically fastened with a clevis-tang joint, each joint having two 12-ft-diameter continuous O-ring seals (see fig. 1(b)). The joints connecting four case segments together in the field, utilizing two O-rings, are designated field joints. The joints connecting two case segments together in the factory, utilizing two O-rings and a continuous layer of internal insulation, are designated factory joints. An investigation by the Presidential Commission on the Challenger accident concluded that "the cause of the Challenger accident was the failure of the pressure seal in the aft field joint of the Solid Rocket Motor" (ref. 1). The Commission also stated that the elastomeric seals were severely affected (hardened) by the low temperatures at launch. As a result, the field joints of the solid rocket motor (SRM) were redesigned (see fig. 2) in accordance with the Prime Equipment Contract End Item Detail Specification (ref. 2).

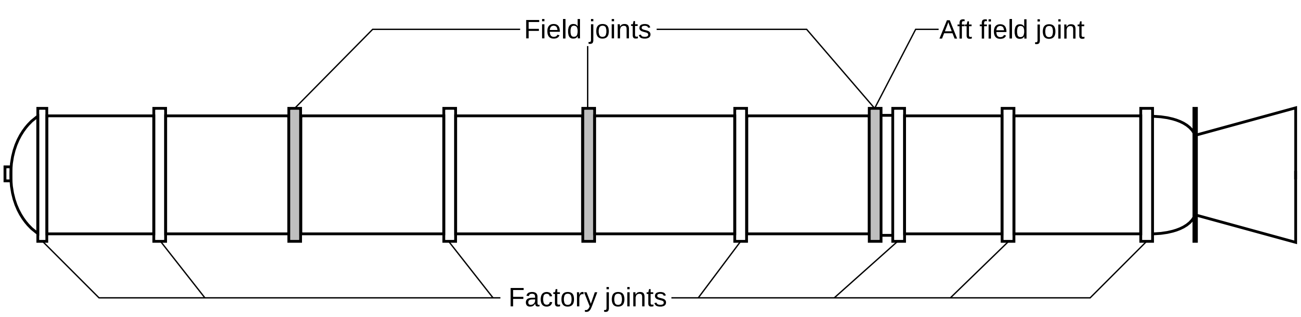

(a) Space Shuttle SRB.

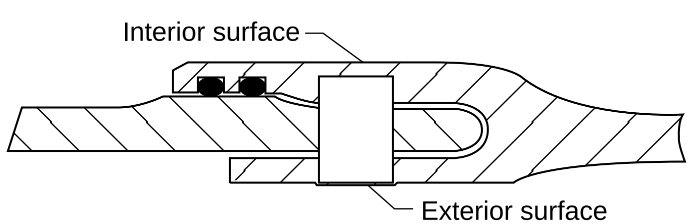

(b) Original field joint.

Figure 1. Schematic of Space Shuttle SRB and original field joint detail.

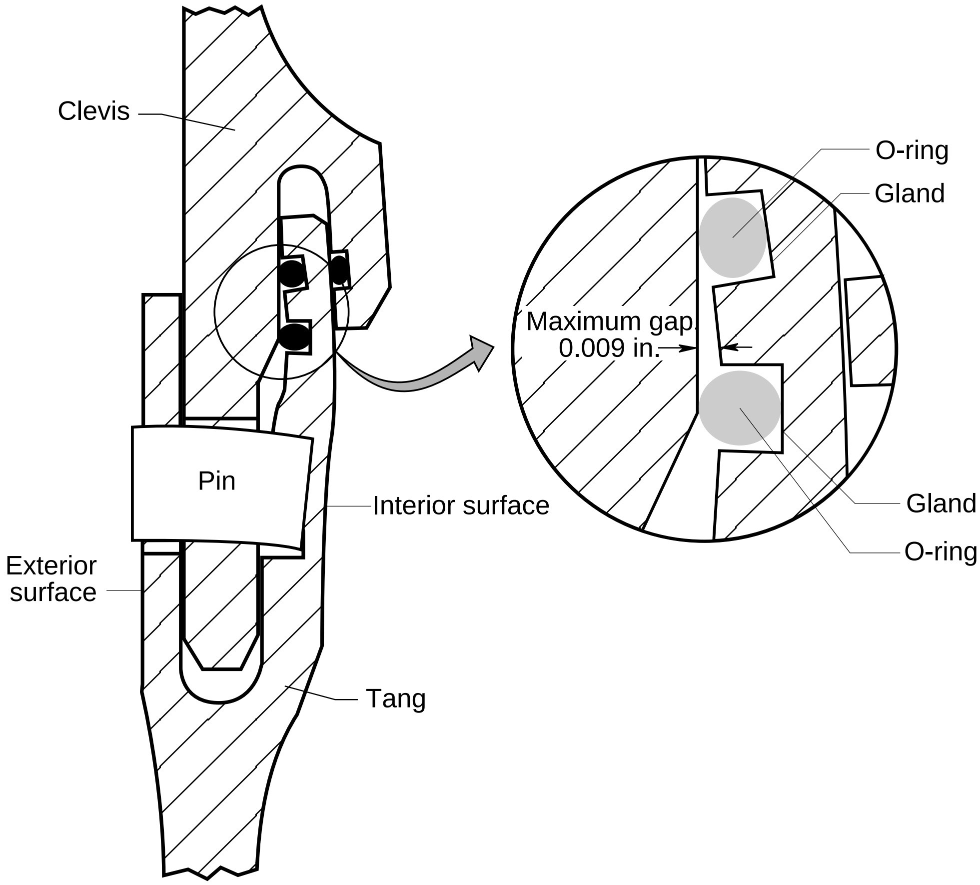

Figure 2. Schematic of redesigned field joint showing location of maximum gap opening during internal SRB pressurization.

The two main sources of SRB joint structural deflections are the dynamic external tank (ET)/SRB attach strut loads during Shuttle launch and the internal pressurization of the SRB during ignition. The structural deflections associated with the attach strut are caused by the constraint of the SRB during Shuttle main motor ignition. These constraint loads are stored within the assembled structure and released immediately after Shuttle launch. An analysis of previous flight data revealed that the structural vibrations caused by the attach strut loads produce maximum joint gap deflections of 0.001 in. at 3 Hz (private communication from Frank Bugg of NASA Marshall Space Flight Center, January 1987). The second source of deflection is the internal motor pressurization of the SRB. The 3σ case of the head end SRB motor pressure would result in a maximum internal pressure of 1015 psi. This pressure will create a maximum gap opening (delta gap) of 0.009 in. between the clevis and the tang of the redesigned field joint as shown in figure 2 (ref. 3).

The primary requirements for the seals in the redesigned field and nozzle-to-case joints are as follows: the seal must operate within a specified temperature range, any structural deflections must be accommodated, the O-ring seal must be capable of tracking twice the maximum expected gap opening without pressure assistance, and the use of pressure assistance for sealing must be possible but not required.

This investigation examined the resiliency characteristics of five candidate SRB O-ring materials in the redesigned gland (groove housing the O-ring). The five candidate materials consisted of Viton V747-75, which was the original O-ring material (used on all previous Shuttle launches), and four alternates: modified fluorocarbon V835-75, nitrile N304-75 and N602-70, and silicone S650-70. The following two types of tests were conducted: resiliency characterization tests to examine the response of the O-ring at various gap opening rates for various temperatures, and joint deflection tests to verify the ability of the O-ring to track the prescribed gap opening and vibrations without pressure assistance. For the joint deflection tests, a computer generated the nonlinear displacement gap opening to verify the resiliency response at twice the maximum expected gap opening (i.e., 2×0.009 in. = 0.018 in.).

Test Equipment and Procedures

The O-ring tests were conducted in a face seal test fixture mounted in a servo-hydraulic test machine. The face seal fixture squeezed the O-ring in a direction normal to the plane containing the O-ring (see fig. 3). The face seal fixture contained a gland that was fabricated with the cross-sectional dimensions of the redesigned field joint gland. During each test, normal forces on the O-rings were measured with a load cell while a direct-current displacement transducer (DCDT) measured the separation distance between the fixture halves. Thermocouples were used to verify that thermal equilibrium of the test fixture halves was maintained at the desired test temperature.

Prior to testing, the O-rings and the fixture glands were lightly covered with the calcium-based grease used in the SRB gland for corrosion protection and O-ring lubrication. The O-rings were placed in the fixture halves and compressed to an initial gap separating the fixture halves that related to a given percent squeeze (the amount of diametral compression) of the O-ring. The fixture halves were held at this initial gap for approximately 30 min to allow for viscoelastic relaxation. The relaxation relieved the peak load resulting from the initial compression. This relaxation process was possible in the redesigned gland because, when compressed, the O-rings were not constrained by the sidewalls of the gland. This was necessary to incorporate the redesign requirement of accommodating but not requiring pressure assistance.

The minimum load determined at the end of the relaxation period is referred to as the "relaxed" load. During the 30-min relaxation period, the fixture halves were brought to the desired test temperature. In order to expedite consecutive tests, new O-rings at room temperature were placed in the fixture halves, which were already at the specified test temperature. The O-rings were immediately compressed to allow for the viscoelastic relaxation effects before thermal equilibrium was established between the O-ring and the fixture. A 30-min relaxation period was then observed.

The O-rings for the resiliency characterization tests had an inner diameter of 4.477 in. and a nominal cross-sectional diameter of 0.280 in. (preliminary SRB redesign size). The resiliency behavior of all five of the candidate O-ring materials was examined (see table I for the respective material properties).

Table I. Candidate O-Ring Material Properties

Elastomeric material	Glass transition temperature,[1] °F		Dynamic storage moduli,[2] psi (rate 10 rad/sec)			Coefficient of thermal expansion,[3] μin/in-°F
	No grease	With grease	14°F	68°F	122°F	Range: 32°F–212°F
Viton V747-75	9	9	26706	2094	1555	80
Modified fluorocarbon V835–75	−15	−13	5610	2610	2240	98
Nitrile N304-75	−65					64
Nitrile N602-70	−45	7	3361	1968	1481	104
Silicone S650-70	−143	−141	2630	1860	1470	

[1]Reference 4, calculated by the TMA method.

[2]Reference 7.

[3]Reference 8.

(a) Photograph of lower half of face seal fixture.

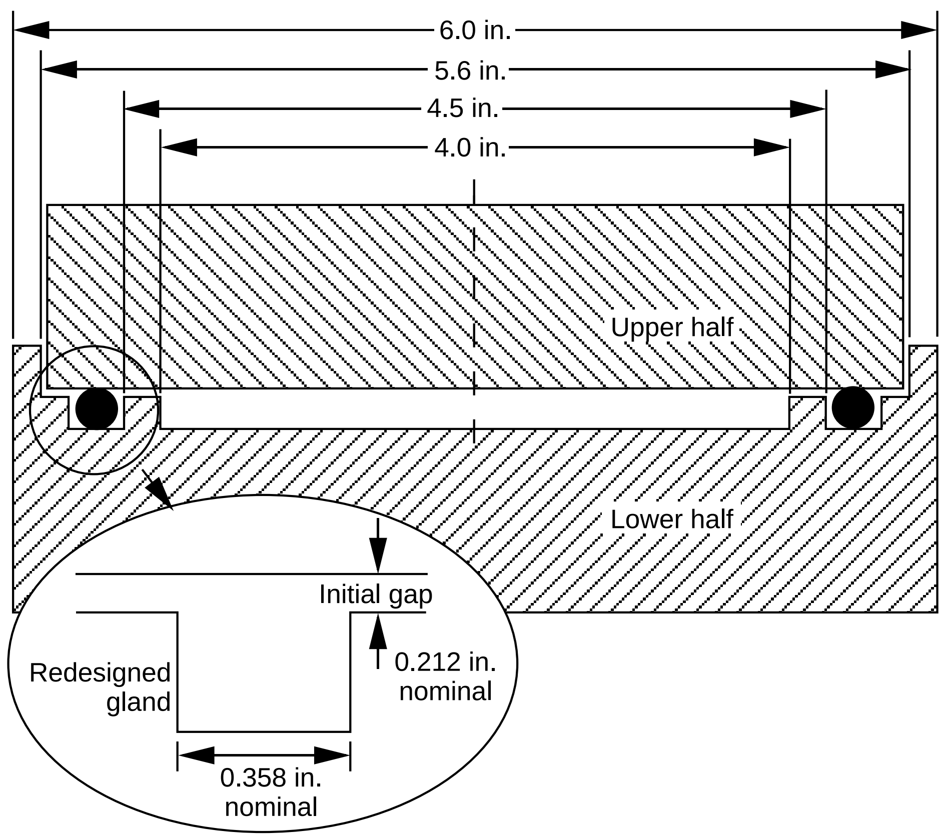

(b) Schematic of face seal fixture.

Figure 3. Photograph and schematic of face seal fixture used for resiliency tests.

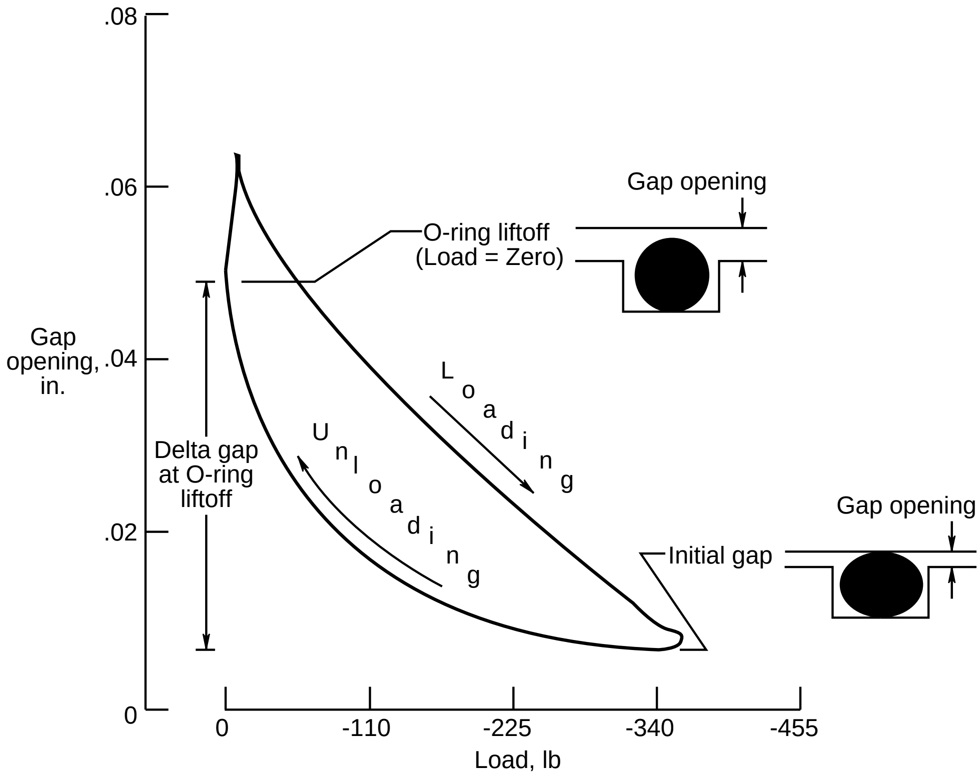

Figure 4. Format of O-ring resiliency test data.

The simulated SRB field joint deflection tests used the same face seal fixture (see fig. 3) as the resiliency characterization studies but used a servo-hydraulic test machine that provided better displacement response times to accommodate the simulated joint displacement history. The test O-rings had a nominal cross-sectional diameter of 0.290 in. (final SRB redesign size) and a nominal inner diameter of 4.477 in. For this study, three candidate O-ring materials were tested: Viton V747-75, modified fluorocarbon V835-75, and silicone S650-70*. The asterisk on the silicone designation indicates that the material was preconditioned by baking the O-ring in a bed of calcium-based grease until it was saturated. The nitrile elastomers, N304-75 and N602-70, were not tested, primarily because of the long-term detrimental effects caused by grease absorption and compression set. Results from other characterization tests in reference 4, which included high-temperature sealing, dynamic pressurization, and mechanical properties, further downgraded nitrile as a candidate material.

Resiliency Characterization Test Procedure

During the test preparations, the O-ring was compressed so that the initial gap separating the fixture halves was 0.005 in., which corresponds to a 22.5-percent squeeze. The lower fixture half was then cyclically displaced at various frequencies to produce a load versus displacement hysteresis as shown in figure 4. A cyclic displacement was chosen with sufficient amplitude such that the O-ring would eventually lose contact with the sealing surface. The cyclic displacements were converted to gap opening rates to determine the response of the O-ring in relation to operational gap opening rates. Figure 4 shows the delta gap at O-ring liftoff as the difference between the initial gap separating the fixture halves and the gap opening when the O-ring is no longer in contact with the sealing surface. These tests were conducted at several constant temperatures between 20°F and 120°F. The cyclic displacements followed a prescribed sine wave at frequencies ranging from 0.01 Hz to 50 Hz.

Simulated SRB Field Joint Deflection Test Procedure

The O-ring was initially compressed to either 16.2- or 23.3-percent squeeze (which corresponded to an initial gap of 0.031 in. and 0.010 in., respectively) followed by a relaxation period. These values of squeeze from reference 4 were incorporated into the redesign requirements and represent variations in factors such as stretch, thermal expansion, and estimated long-term compression set effects.

A computer generated the nonlinear displacement gap opening that simulated twice the maximum gap opening curve resulting from the 3σ pressurization of the SRB field joint. Figure 5 shows the computer-generated displacement gap opening and the resulting gap opening displacement of the fixture mounted in the servo-hydraulic machine. The vibrational contributions to the delta gap opening were added onto the end of the computer-generated displacement gap opening (at 600 msec) to determine the effect of the vibrations due to the ET/SRB attach strut loads.

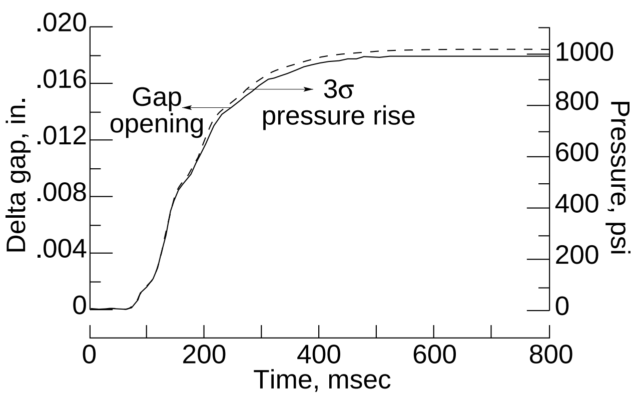

Figure 5. Displacement history and 3σ pressure rise for field joint deflection test.

Two test temperatures were used, 75°F and 120°F, which bracketed the specified operating range of the O-ring seal (ref. 2). Six tests were conducted at each temperature: three for the delta gap only and three with the vibrational contributions added. The minimum load per unit length acting on the O-ring was calculated from the residual load measurements.

Results

Grease affected the performance of the elastomeric material and altered its inherent properties (see table I). In particular, silicone absorbed the calcium grease and swelled, thereby increasing the diameter of the O-rings. Thus, undersized silicone O-rings were preconditioned by baking them in a bed of calcium grease to eliminate further swelling and grease absorption during testing (ref. 5). The other materials did not absorb a significant amount of the calcium grease during short-term testing (ref. 6).

Resiliency Characterization Tests

Figures 6–11 show the resiliency behavior of the five candidate materials at temperatures from 70°F to 20°F in decreasing intervals of 10°F. Each figure has the delta gap at liftoff (the displacement at which the O-ring no longer maintains contact) plotted versus the gap opening rate in inches per second. These plots can be used to determine which O-ring material has the appropriate resiliency for a given gap opening rate as a function of fixed displacement (delta gap at liftoff) and test temperature. For example, in figure 6 at a gap opening rate of 0.3 in/sec silicone S650-70, modified fluorocarbon V835-75, and nitrile N602-70 could accommodate a delta gap opening of 0.025 in., while Nitrile N304-75 and Viton V747-75 could not. In general, the O-ring materials had the same ranking, in terms of resiliency, over the entire temperature range tested. However, as the test temperature decreased, larger differences in resiliency between the individual materials were observed. For a given test temperature, silicone S650-70 was consistently the most resilient, while Viton V747-75 was the least. In fact, Viton V747-75 became totally unresponsive to gap opening rates and delta gap openings at 20°F.

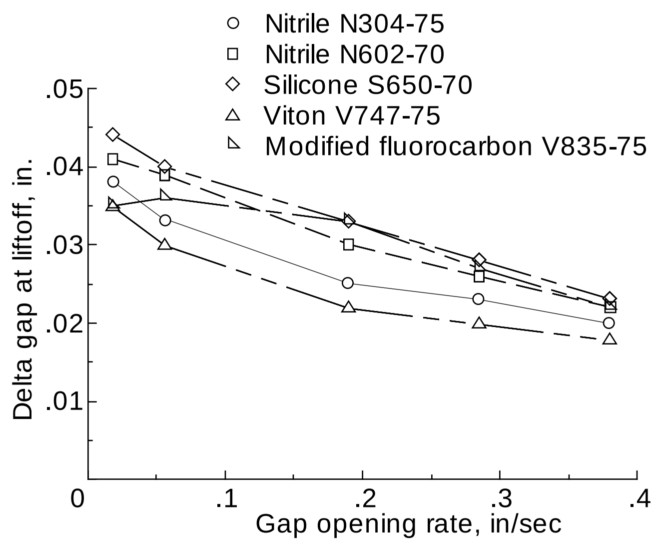

Figure 6. Resiliency behavior of candidate O-ring materials at 70°F.

Simulated SRB Field Joint Deflection Tests

Typical results from an SRB field joint deflection test are shown in figure 12. Figure 12(a) shows the displacement (delta gap opening) of the fixture within the 600-msec time frame of the computer-generated displacement gap opening. The 3-Hz, ±0.0005-in. vibrations were added at 600 msec at the end of the displacement gap opening. The fixture

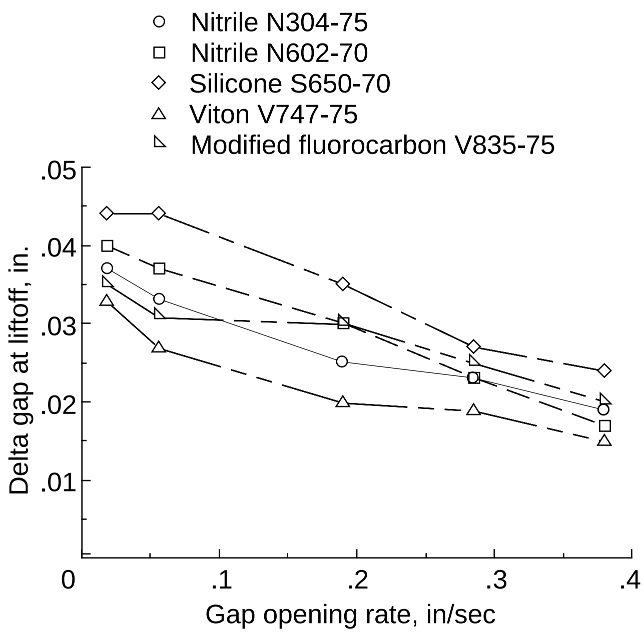

Figure 7. Resiliency behavior of candidate O-ring materials at 60°F.

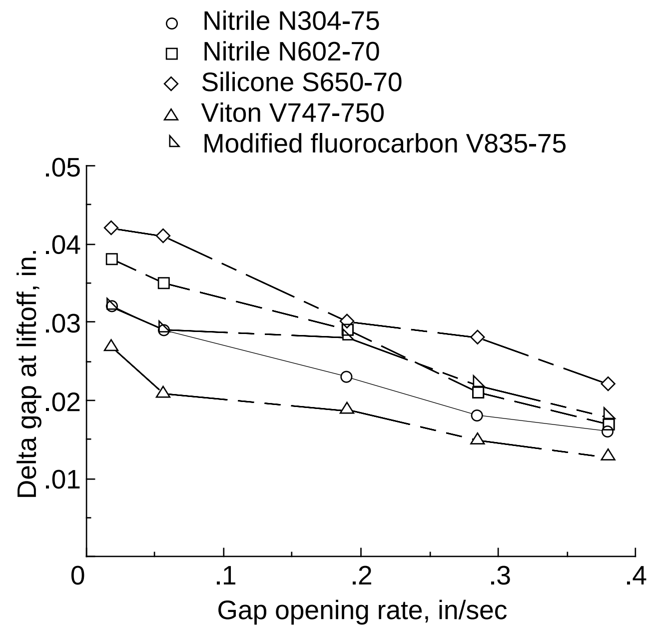

Figure 8. Resiliency behavior of candidate O-ring materials at 50°F.

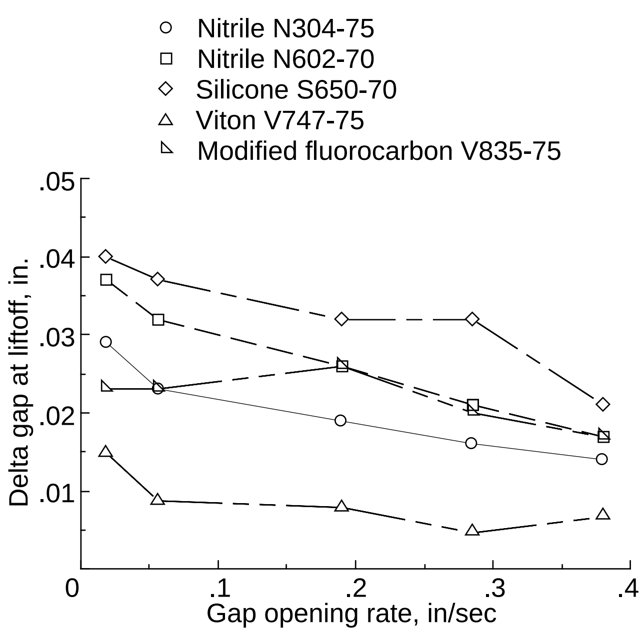

Figure 9. Resiliency behavior of candidate O-ring materials at 40°F.

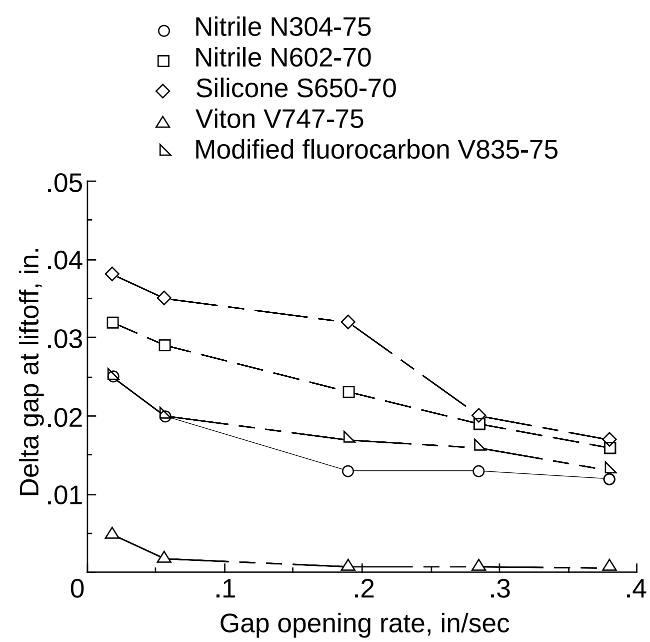

Figure 10. Resiliency behavior of candidate O-ring materials at 30°F.

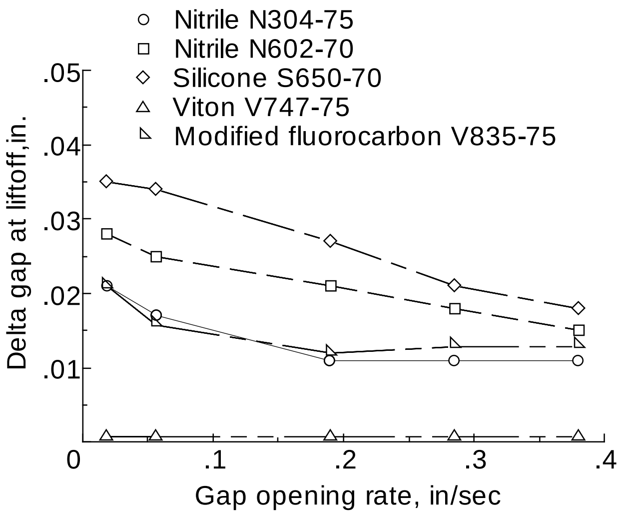

Figure 11. Resiliency behavior of candidate O-ring materials at 20°F.

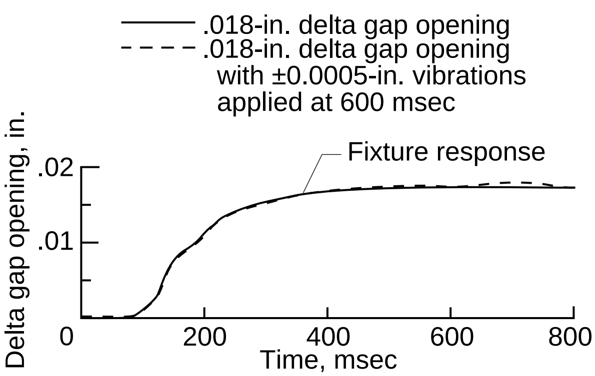

(a) Displacement response of fixture to programmed delta gap openings.

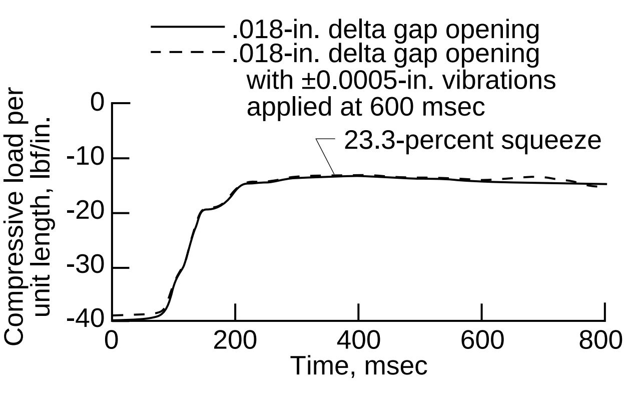

(b) Compressive load trace.

Figure 12. Results from simulated SRB field joint deflection test for V747-75 at 75°F.

response followed the computer-generated displacement gap opening very closely, with a maximum error in delta gap opening of 0.001 in. The error in the final delta gap opening of 0.018 in. was much smaller. An example of the resiliency response of Viton V747-75 at 75°F is shown in figure 12(b). The compressive load per unit length is plotted against the 600-msec time frame corresponding to the computer-generated displacement gap opening. Viton maintained contact throughout the computer-generated displacement gap opening and the computer-generated displacement gap opening with the vibrational contributions added at 600 msec, as shown by the compressive load curve in figure 12(b). Note that the resulting compressive load curve follows every change in slope of the computer-generated displacement gap opening.

Discussion

Although the O-rings were statically compressed for approximately 30 min, the majority of the relaxation occurred within 4 min; during this time the O-ring typically lost 28 percent of its original load. The load further reduced only 5 percent by the end of the relaxation period. The changes in the load state (viscoelastic relaxation) were a result of the O-ring being unconstrained by the sidewalls of the gland; this unloading occurred before thermal equilibrium between the O-ring and the fixture was established.

The viscoelastic relaxation period for these tests did not induce the permanent compression set that the SRB O-rings would experience during storage after assembly. Compression set is the unrecovered deformation (as a fraction of the original squeeze) that the O-ring experiences after being held in compression for an extended period of time. Compression set alters the O-ring resiliency. Thus, these short-term tests only revealed the basic effect of temperature on the resiliency of the elastomer.

Resiliency Characterization Tests

Figures 6–11 show the resiliency behavior of the five candidate materials at temperatures from 70°F to 20°F in decreasing intervals of 10°F. The ability of the O-ring to track the gap opening displacement (resiliency) decreased at lower temperatures and higher gap opening rates. Silicone S650-70 exhibited the best resiliency over the entire temperature range and was only mildly affected by the lower temperatures. In contrast, the resiliency of Viton V747-75 was severely reduced with decreasing temperature, particularly at the lowest temperature of 20°F, where the Viton O-ring lifted off immediately, regardless of the gap opening rate. Since the 20°F test temperature was much closer to the glass transition temperature of Viton V747-75 than that of the other candidate materials tested, the largest effect was expected for Viton, which was shown to be much stiffer at the lower temperatures (ref. 7) (see table I). The thermal ranking of the candidate O-ring materials was in accordance with the results from tests performed at Marshall Space Flight Center (ref. 8).

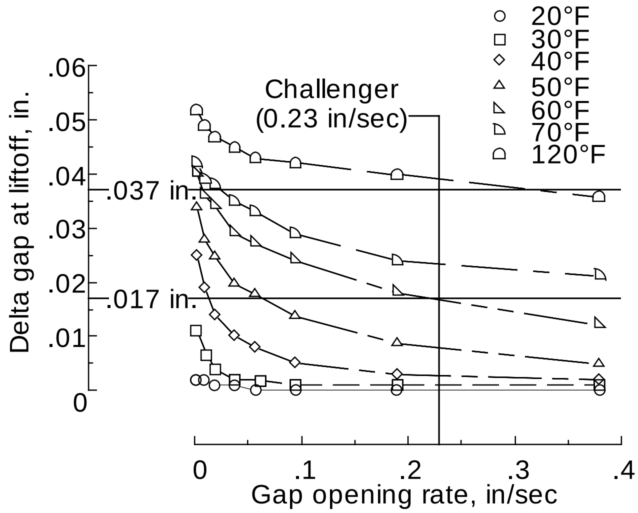

Figure 13. Viton response at Challenger's joint deflection and gap opening rate.

In order to characterize the full resiliency behavior of Viton V747-75, additional testing was performed that included a test temperature of 120°F and gap opening rates less than 0.1 in/sec. The results are shown in figures 13 and 14. Figure 13 shows that the resiliency of the Viton V747-75, which was used on the Challenger flight, was adversely affected by cold temperatures, particularly in the range of expected gap opening rates for the original field joint (0.23 in/sec) (ref. 9). Various structural analyses of the original SRB field joint showed that the average gap or relative displacement between tang and inner clevis arm ranged from 0.017 to 0.037 in. (refs. 1, 10, and 11). For the original SRB field joint, the estimated maximum gap opening rate of 0.23 in/sec was calculated from data provided in reference 11. At the mean joint launch temperature of Challenger, 28°F, the Viton V747-75 O-ring was unable to track the delta gap opening (0.017–0.037 in.) at the prescribed rate of 0.023 in/sec, nor could it track the maximum displacement requirement of 0.018 in. at a gap opening rate of 0.019 in/sec as required for the redesigned joint (see fig. 14). This investigation also confirms the Presidential Commission findings on the Challenger accident (ref. 1).

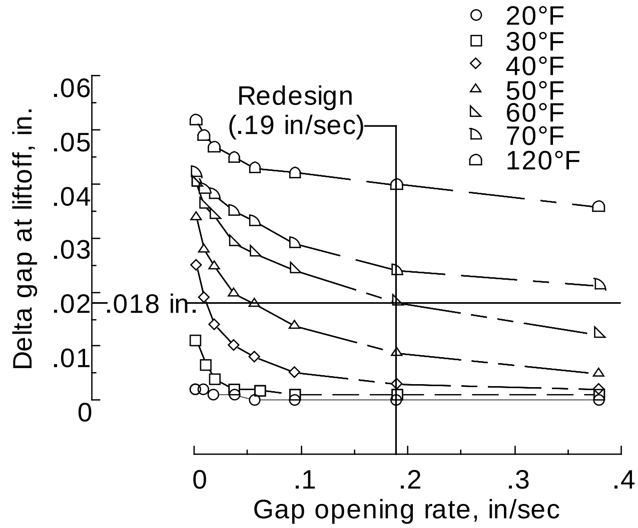

Figure 14. Viton response at redesign joint deflection and gap opening rate.

Simulated SRB Field Joint Deflection Tests

Figures 15 and 16 show the results of the tests simulating structural deflections of the SRB field joint. The most significant feature of the results is that the compressive load on the O-ring did not drop to zero during the simulation, indicating that the O-ring successfully tracked the delta gap opening and maintained contact with the sealing surface. For all materials, initial squeezes, and temperatures tested, the O-ring tracked the required gap opening of 0.018 in. without pressure assistance during the critical 600-msec interval.

In addition to verifying that the O-ring materials could track the delta gap, it was of interest to assess the effects of the test variables on the minimum residual loads on the O-rings at the maximum gap. The magnitude of the residual load is a measure of the sealing capability of the O-ring; the higher the load the better the seal. Figures 15 and 16 show the effects of O-ring material, temperature, and vibrations on the residual loads for initial squeezes of 16.2 and 23.3 percent, respectively. The trends for the two squeezes were very similar, but the higher initial squeeze resulted in higher residual loads. The modified fluorocarbon V835-75 exhibited the highest residual loads at all test conditions, and the silicone S650-70* exhibited the lowest loads.

The higher residual loads for all materials at 120°F in comparison to those at 75°F (figs. 15 and 16) are most probably caused by thermal expansion. The difference was largest for modified

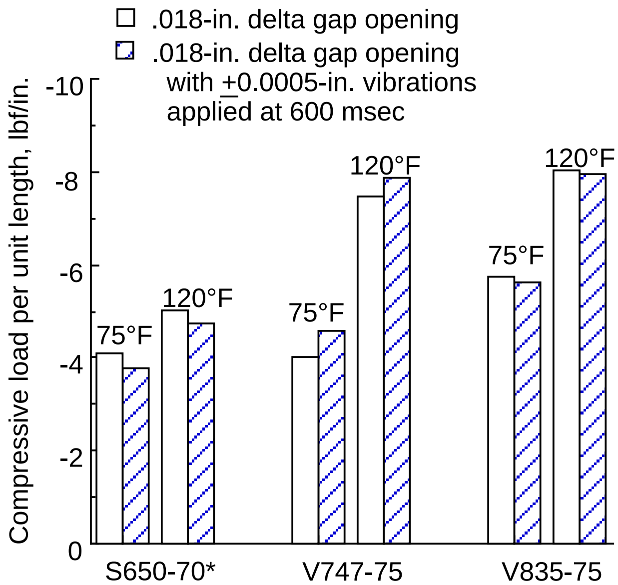

Figure 15. Residual load values of candidate materials at 16.2-percent squeeze at 75°F and 120°F.

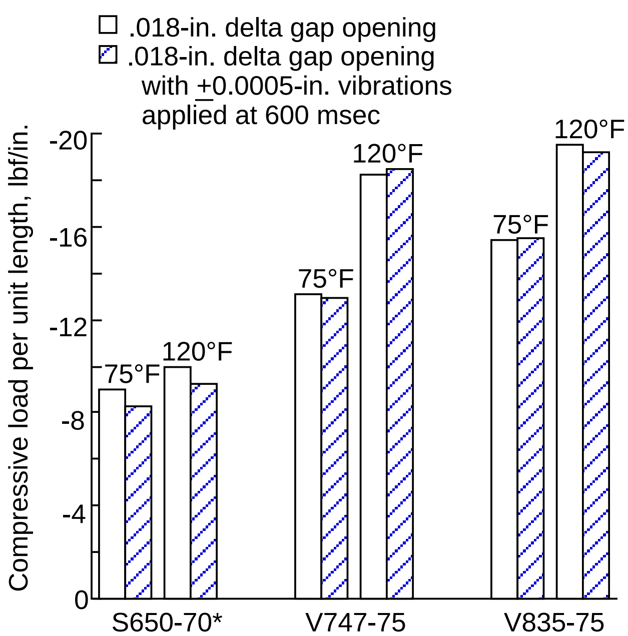

Figure 16. Residual load values of candidate materials at 23.3-percent squeeze at 75°F and 120°F.

fluorocarbon V835-75 because it had the highest coefficient of thermal expansion, which created additional compressive stresses when the O-ring was in a restrained position within the face seal fixture. In contrast, silicone S650-70* had the smallest change in load with respect to temperature change. A combination of low thermal expansion coefficient and grease probably resulted in the small change. The grease is known to reduce the dynamic storage modulus of silicone S650-70* and hence the residual load capacity (ref. 4) (see table I).

Figures 15 and 16 also indicate that the effects of vibration on residual load are minimal for all the materials in each test condition. Although the 3-Hz, ±0.0005-in. vibrations generally decreased the residual loads, the added vibrations did not result in the O-rings losing contact with the sealing surface at any time. The silicone S650-70*, having the lowest dynamic storage modulus of all the candidate materials, showed the greatest loss in residual load with the vibrations added.

Summary of Results

Resiliency tests were conducted to assess O-ring sealing capability with regard to the revised solid rocket booster (SRB) seal requirements. The effects of temperature and gap opening rates were determined. Additional resiliency tests were conducted to investigate the various O-ring responses to simulated SRB field joint deflections. Resiliency was gauged by load and displacement measurements. All tests were conducted in a face seal fixture that was mounted in servo-hydraulic test machines.

Although the other candidate materials exhibited superior resiliency at lower temperatures, Viton V747-75 was selected as the baseline O-ring for the redesigned SRB's because Viton was the only candidate elastomer chemically inert to calcium grease. The minimum operating temperature at which the Viton V747-75 O-ring can easily track the required gap opening of 0.018 in. at the gap opening rate of 0.19 in/sec is 70°F. In order to guarantee adequate resiliency response from the Viton O-rings, the redesign of the SRB field joints included heaters to maintain a thermal environment of 75°F to 120°F.

Specific findings resulting from this study are as follows:

1. The candidate O-ring materials typically tracked the displacement gap opening better at higher temperatures and lower gap opening rates.
2. Silicone S650-70 had the best resiliency over the temperature range 70°F to 20°F.
3. The resiliency of Viton V747-75 decreased rapidly as the temperature decreased, and at 20°F it immediately lifted off the sealing surface regardless of gap opening rate.
4. The external tank (ET)/SRB vibrational contributions had a negligible effect on the ability of the O-ring to track the delta gap opening.

5. All three of the candidate O-ring materials successfully tracked the delta gap opening in the deflection tests at 75°F and 120°F.

NASA Langley Research Center
Hampton, VA 23665-5225
May 14, 1992

References

1. Presidential Commission on the Space Shuttle Challenger Accident: *Report of the Presidential Commission on the Space Shuttle Challenger Accident,* Volumes I–V. June 6, 1986.

2. Thiokol Corp.: *Performance, Design, and Verification Requirements—Space Shuttle Redesigned Solid Rocket Motor CPW1-3600A for Space Shuttle Solid Rocket Motor Project Operational Flight Motors (360L004 and Subsequent).* Spec. No. CPW1-3600A (Prime Equipment Contract End Item Detail Specification, Part I of Two Parts), Jan. 27, 1992.

3. Thiokol Corp.: *RSRM CDR Summary Report, Seal Design.* TWR-17082 (Contract No. NAS8-30490), Morton Thiokol, Inc., Dec. 21, 1987.

4. Patterson, W. J.: *Alternate Seal Material Characterization for SRM Joint Redesign Grease Compatibility Report.* Test Rep. #MSFC-EH33-87-3, NASA George C. Marshall Space Flight Center, Apr. 1987.

5. Patterson, W. J.: *Alternate Seal Material Characterization for SRM Joint Redesign Compression Set Report.* Test Rep. #MSFC-EH33-87-4, NASA George C. Marshall Space Flight Center, July 1987.

6. Turner, J. E.: Evaluation of the Sealing Ability of Various O-Ring Materials for the Space Shuttle Redesigned Solid Rocket Motor. *1988 JANNAF Structures & Mechanical Behavior Subcommittee Meeting,* CPIA Publ. 490 (Contract N00039-87-C-5301), Applied Physics Lab., Johns Hopkins Univ., June 1988, pp. 25–35.

7. Ledbetter, Frank E., III: *Alternate Seal Material Characterization for SRM Joint Redesign Mechanical Properties Report.* Test Rep. #MSFC-EH33-87-1, NASA George C. Marshall Space Flight Center, Jan. 1987.

8. Morris, Donald E.: *Alternate Seal Material Characterization for SRM Joint Redesign.* Test Rep. #MSFC-EH33-86-1, NASA George C. Marshall Space Flight Center, Dec. 1986.

9. Greene, William H.; Knight, Norman F., Jr.; and Stockwell, Alan E.: *Structural Behavior of the Space Shuttle SRM Tang-Clevis Joint.* NASA TM-89018, 1986.

10. Turner, James E.: *Evaluation of the Sealing Capabilities of Several O-Ring Materials in Subscale, Cold-Gas Pressurization Tests.* NASA TM-86586, 1987.

11. Knight, Norman F., Jr.; Gillian, Ronnie E.; and Nemeth, Michael P.: *Preliminary 2-D Shell Analysis of the Space Shuttle Solid Rocket Booster.* NASA TM-100515, 1988.

REPORT DOCUMENTATION PAGE			Form Approved OMB No. 0704-0188

1. AGENCY USE ONLY *(Leave blank)*	2. REPORT DATE June 1992	3. REPORT TYPE AND DATES COVERED Technical Paper

4. TITLE AND SUBTITLE
Effect of Temperature and Gap Opening Rate on the Resiliency of Candidate Solid Rocket Booster O-Ring Materials

5. FUNDING NUMBERS
WU 505-63-50-03

6. AUTHOR(S)
Cynthia L. Lach

7. PERFORMING ORGANIZATION NAME(S) AND ADDRESS(ES)
NASA Langley Research Center
Hampton, VA 23665-5225

8. PERFORMING ORGANIZATION REPORT NUMBER
L-17023

9. SPONSORING/MONITORING AGENCY NAME(S) AND ADDRESS(ES)
National Aeronautics and Space Administration
Washington, DC 20546-0001

10. SPONSORING/MONITORING AGENCY REPORT NUMBER
NASA TP-3226

11. SUPPLEMENTARY NOTES

12a. DISTRIBUTION/AVAILABILITY STATEMENT
Unclassified–Unlimited

Subject Category 27

12b. DISTRIBUTION CODE

13. ABSTRACT *(Maximum 200 words)*
As a part of the redesign of the Space Shuttle solid rocket motor following the Challenger accident, the field and nozzle-to-case joints were designed to minimize gap opening caused by internal motor pressurization during ignition. The O-ring seals and glands for these joints were designed both to accommodate structural deflections and to promote pressure-assisted sealing. The resiliency behavior of several candidate O-ring materials was evaluated for the effects of temperature and gap opening rates. The performance of three of the elastomeric materials was tested under the specific redesign gap opening requirement. Dynamic flexure conditions unique to launch produce low-frequency vibrations in the gap opening. The effect of these vibrations on the ability of the O-ring to maintain contact with the sealing surface was also addressed. The resiliency of the O-ring materials was found to be extremely sensitive to variations in temperature and gap opening rate. The top three elastomeric materials tracked the simulated solid rocket booster (SRB) field joint deflection at 75°F and 120°F. The external tank/SRB attach strut load vibrations had a negligible effect on the ability of the O-ring to track the simulated SRB field joint deflection.

14. SUBJECT TERMS
O-ring; Seal; Resiliency; Viton; Elastomers

15. NUMBER OF PAGES
12

16. PRICE CODE
A03

17. SECURITY CLASSIFICATION OF REPORT	18. SECURITY CLASSIFICATION OF THIS PAGE	19. SECURITY CLASSIFICATION OF ABSTRACT	20. LIMITATION OF ABSTRACT
Unclassified	Unclassified		